Chapter 15

Ionosphere Critical Frequency

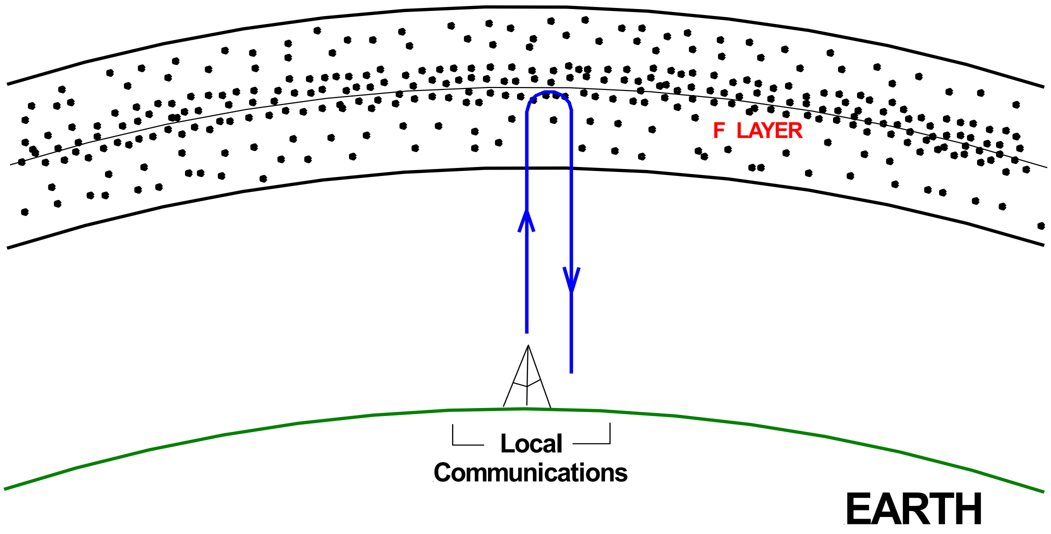

15 Critical Frequency

The primary phenomena affecting propagation of radio waves through the ionosphere are:

- Critical frequency,
- Maximum usable frequency,
- Skip distance,
- Signal fading and noise,
- Propagation modes, and
- Ionospheric storms

These topics are covered in the net few chapters beginning with critical frequency in this chapter.

Critical frequency is very important. Critical frequency determines:

- What frequency bands are open and when,
- The maximum usable frequency (MUF) for communicating with other stations,
- Whether a skip zone exists, and if so how large it is,
- Whether Near Vertical Incident Skywave (NVIS) propagation is possible or not,
- The performance of Regional and Local HF nets, specifically what stations can be reached, which cannot, plus the strategy for positioning net control stations,
- And more

Critical Frequency f_c is the highest frequency signal that can be transmitted straight up and reflected back down to Earth, illustrated by the blue trace in Figure 1. All signals lower in frequency than f_c will also be reflected back to Earth. But, signals higher in frequency transmitted straight up will penetrate the ionosphere and be lost to outer space as illustrated by the brown trace in Figure 1.

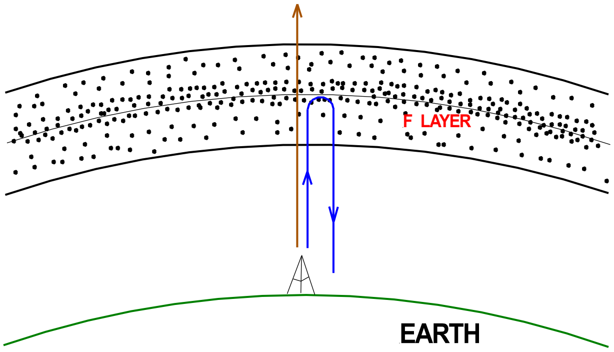

Figure 1 Critical frequency (source: author)

15.1 Plasma Frequency

Free electrons and ions are not stationary. Instead, they are in constant motion. In addition, electrostatic forces between positive ions and negative electrons cause electrons to oscillate back and forth in simple harmonic motion around ions. Ions are too massive to oscillate back and forth. Ions are 20,000 times more massive than electrons. The frequency of oscillation, called the plasma frequency, is

$$\omega^2 = \frac{N(h) \cdot e^2}{\varepsilon_0 m}$$

where

ω = angular frequency (radians per second)

N(h) = electron density per cm^3 at an altitude h above Earth's surface

e = electrical charge on an electron

ε_0 = permittivity of free space

m = mass of an electron

Converting from radians per second ω to hertz f

$$f = \frac{\omega}{2\pi}$$

and substituting in the values for the constants e, ε_0, and m, plus changing to MHz gives

$$Plasma\ Freq = f \approx 9(10^{-3})\sqrt{N(h)}\ MHz$$

Plasma frequency is approximately equal to the ionosphere's resonant frequency.

15.2 Regions of the Ionosphere

The regions of the ionosphere and their associated electron densities are shown in Figure 2. The E, F1, and F2 regions each has its own critical frequency.

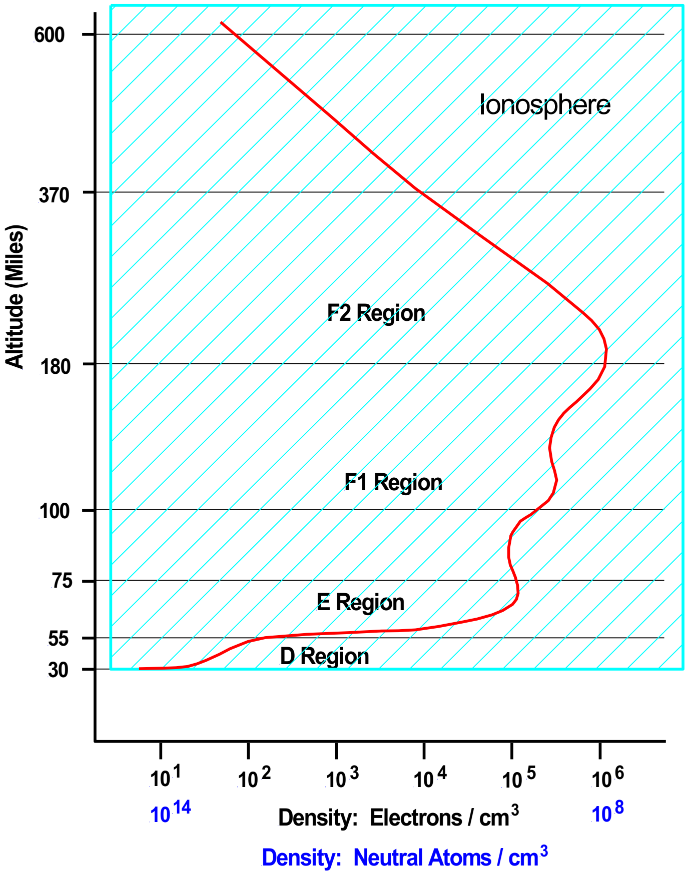

Figure 2 Ionospheric electron density profile (source: author)

The critical frequency for a particular region occurs at the altitude h where its electron density N(h) is maximum. For example, in the F2 region the maximum density is typically 10^6 electrons per cubic centimeter at an altitude of 180 miles (~290 km) as illustrated in Figure 2. This density produces a F2 critical frequency of

$$f_{cF2} = 9(10^{-3})\sqrt{N_{F2}(h)} = 9\ MHz$$

If the maximum electron densities for the E, F1, and F2 regions are respectively

- $N_E = 2 \times 10^5$,
- $N_{F1} = 5 \times 10^5$, and
- $N_{F2} = 1 \times 10^6$

then the critical frequencies are

- f_cE = 4 MHz
- f_cF1 = 6.6 MHz, and
- f_cF2 = 9 MHz

A vertical 4 MHz signal will be reflected back to Earth by the E region. A 6.6 MHz signal will pass through the E region and be reflected back to Earth in the F1 layer. A 9 MHz signal will pass through both E and F1 and reflect back to Earth from the F2 region. A vertical 10 MHz signal will pass through the ionosphere and be lost to outer space.

15.3 Critical Frequency Varies

Critical Frequency varies throughout the day as the Earth rotates, seasonally as the Earth's upper atmosphere changes, and with the 11-year solar cycle as Extreme Ultra-Violate (EUV) and X-ray radiation from the Sun changes.

15.3.1 Diurnal Variations in Critical Frequencies

Diurnal variations are clearly visible in the ionosphere electron density profile shown in Figure 3. Discrete F2, F1, E and D regions are formed during the day (the red and light blue traces in Figure 3). However, at night (the purple and dark blue traces) electron-ion recombination cause the D region to disappear. For most practical purposes, the E region also disappears. The F1 and F2 regions merge forming a weak night time F region as illustrated in Figure 4.

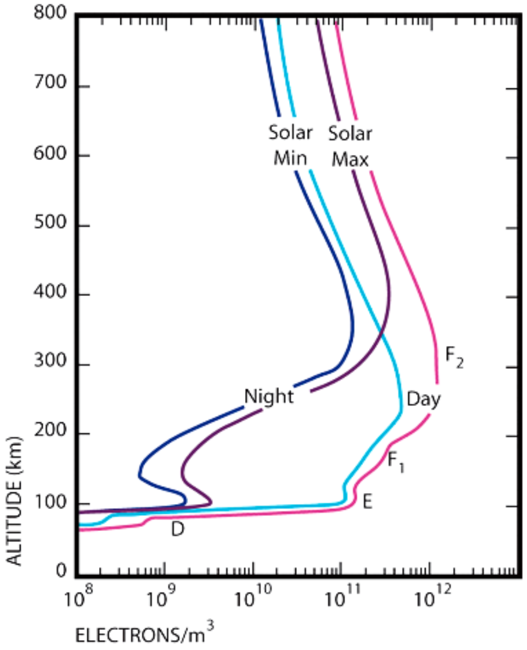

Figure 3 Day vs night ionization levels (source: QSL.net)

Notice that electron concentrations are higher during solar maximum (the red and purple traces) than during solar minimum (light blue and dark blue).

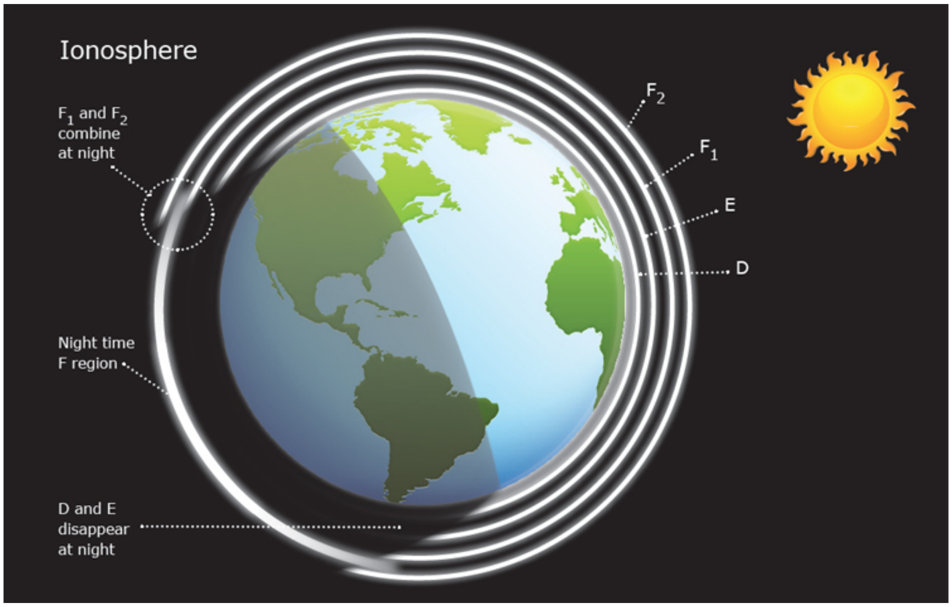

Figure 4 Diurnal variations in ionosphere (source: University of Waikato, www.sciencelearn.org.nz)

F2 critical frequency quickly increases following sunrise until around 10 AM to noon when it plateaus as electron production and recombination rates reach equilibrium. In the winter, during solar maximum, the F2 region reaches its highest critical frequency around noon with critical frequencies typically from 9 – 12 MHz, as illustrated in Figure 5. It then declines in the late afternoon and throughout the evening as electron production decreases and finally stops. During solar minimum F2 critical frequency peaks around noon, levels off or slightly declines, and then peaks again at a higher frequency of around 5 – 6 MHz in the late afternoon, as illustrated in Figures 6.

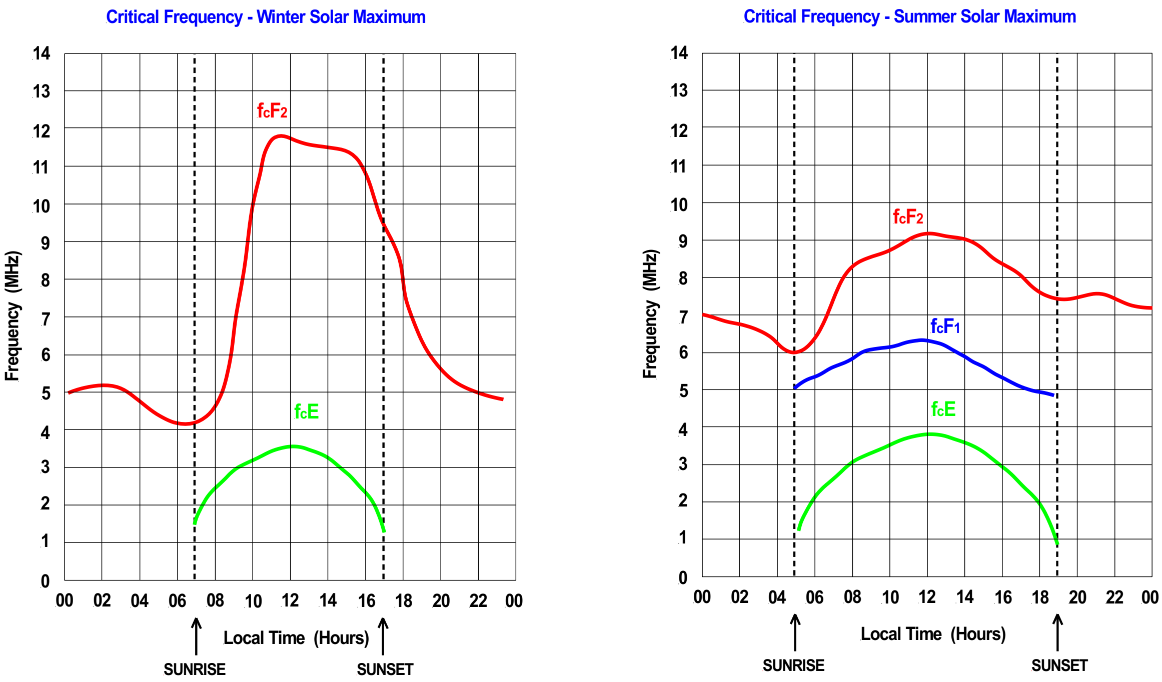

Figure 5 Winter and summer critical frequencies during solar maximum (source: author)

At night the F1 and F2 regions combine forming a single F region. Ionization ceases at night, due to the lack of sunlight, while recombination continues. Consequently, electron density and F critical frequency decline throughout the night. F region critical frequency drops to its lowest level just before sunrise with f_cF around 2 – 3 MHz during solar minimum (Figure 6) and 4 – 6 MHz during solar maximum (Figure 5).

During the day the F1 and E critical frequencies behave similar to Chapman layers (Figure 5 and Figure 6). The E region critical frequency increases rapidly following sunrise, peaks at local noon, and declines in the afternoon. The F1 region acts similarly with the exception of winter during solar maximum when the F1 region disappears. At night, the F1 region merges with the F2 region forming a single F layer. The E region does not completely disappear at night. At night $F_cE \sim 0.6$ MHz, a value which is too low to have any significant effect on HF communications. Thus, for practical purposes we assume that the E region also disappears at night.

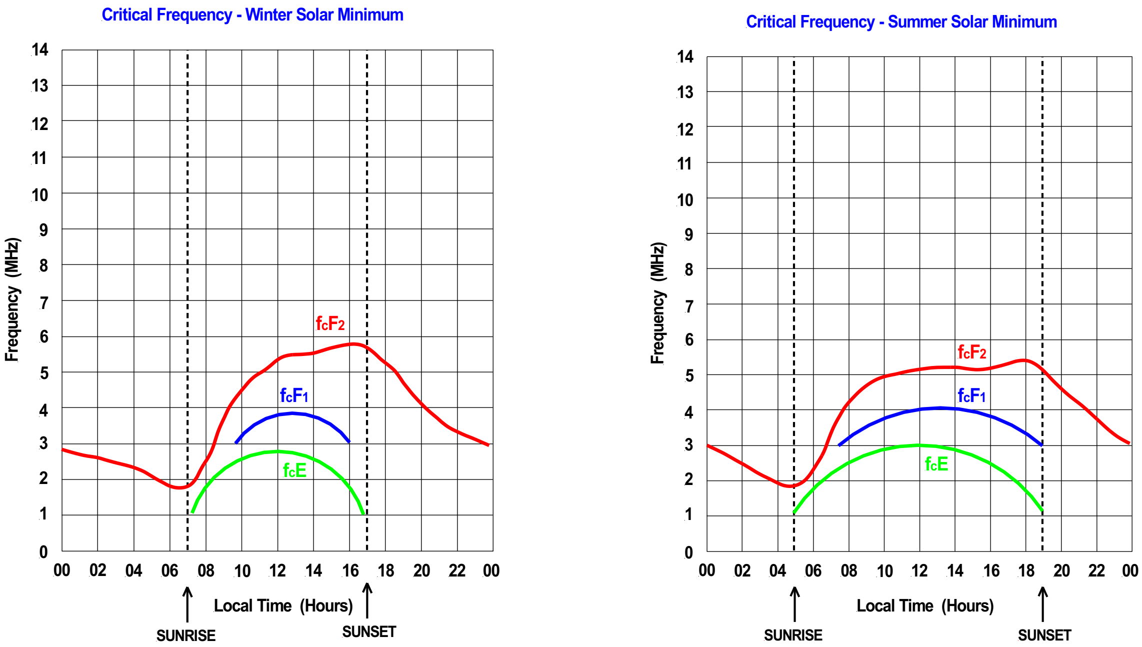

Figure 6 Winter and summer critical frequencies during solar minimum (source: author)

Critical frequency for the E region, at a particular latitude and time of day, is approximately given by the equation

$$f_cE = 0.9 \, [\, (180 + 1.44 \, R) \cos Z \,]^{1/4} \text{ MHz}$$

Similarly, the critical frequency for the F1 region, at a particular latitude and time of day, is given approximately by the equation

$$f_cF1 = (4.3 + 0.01 \, R)(\cos Z \,)^{0.2} \text{ MHz}$$

where R is the current smoothed sunspot number (SSN) and Z is zenith angle at the latitude and time of day of interest.

The current smoothed sunspot number (R = SSN) is shown under “Current Conditions > Space Weather Conditions” on the website www.skywave-radio.org. cos Z is found under “Tools > Solar Position Calculator” on the website

Zenith angle is the angle of the Sun relative to vertical at a particular time of day and location on the Earth’s surface, as illustrated in Figure 7. The zenith angle is 0° when the Sun is directly overhead. At sunrise and sunset the zenith angle is near 90°. Local noon is defined as the time of day when the zenith angle is at a minimum.

At local noon on September 23 and March 21 (the equinoxes) the Sun is directly overhead at the equator. At noon on these two days the zenith angle at the equator is 0^0. At noon on December 21 the zenith angle is 0° at the Tropic of Capricorn. Similarly, at noon on June 21 the zenith angle is 0° on the Tropic of Cancer. Outside of the tropics (bounded by the Tropic of Cancer and the Tropic of Capricorn) the noon zenith angle can never be 0°. The noon time zenith angle must always be greater than 0° in the mid and polar latitudes.

The zenith angles for Los Angeles, CA throughout the day on August 26, 2020 is shown in Figure 8. Note that the zenith angle is lowest a noon (24.0°). The Latitude for Los Angeles is N 34 degrees. On this particular day sunrise occurred at 05:23 and sunset occurred at 18:26.

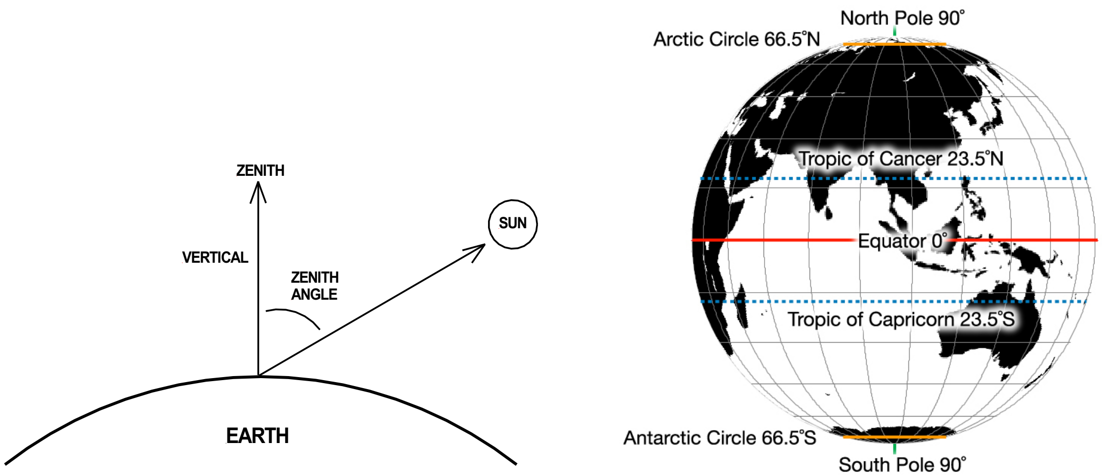

Figure 7 Zenith angle (source: author and ICSM)

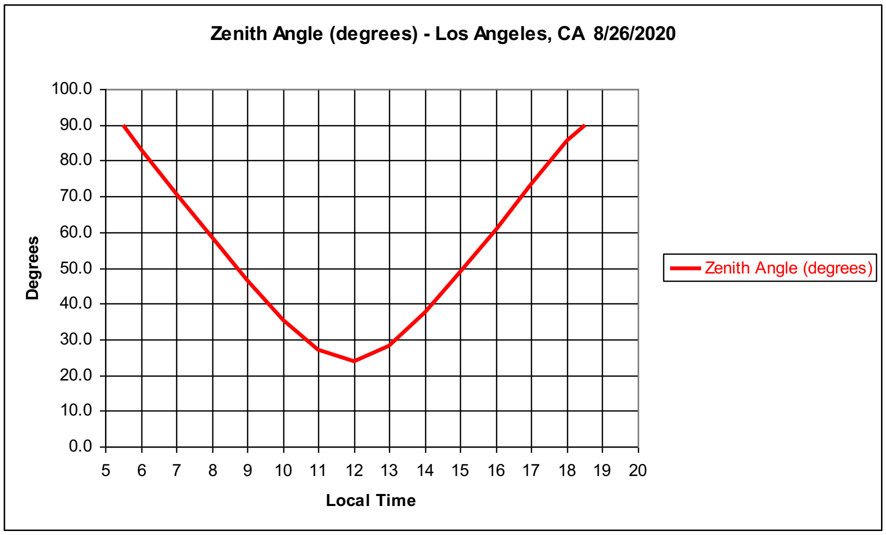

Local Time (hour)	Zenith Angle (degrees)
5.5	90.0
6	83.1
7	70.8
8	58.5
9	46.5
10	35.5
11	27.1
12	24.0
13	28.3
14	37.4
15	48.7
16	60.8
17	73.2
18	85.4
18.5	90.0

Figure 8 Los Angeles zenith angle example (source: author)

Critical frequencies for the F2 region are far more complex than that for the E and F1 regions. The best way to determine the F2 critical frequency is graphically.

The Australian Bureau of Meteorology produces a global F2 critical frequency map that is available on the www.skywave-radio.org website. The critical frequency map is updated every 15 minutes. The map is created automatically from reports received from ionosonde monitoring stations around the world. Seasonal Variations: the shape of f_c profiles are different in the Northern Hemisphere (winter) than in the Southern Hemisphere (summer).

Figure 9 is the Critical Frequency map for January 31, 2024 at 03:00 UT. Over California the critical frequency was between 4 to 5 MHz while critical frequency in Northern Europe was 2 MHz.

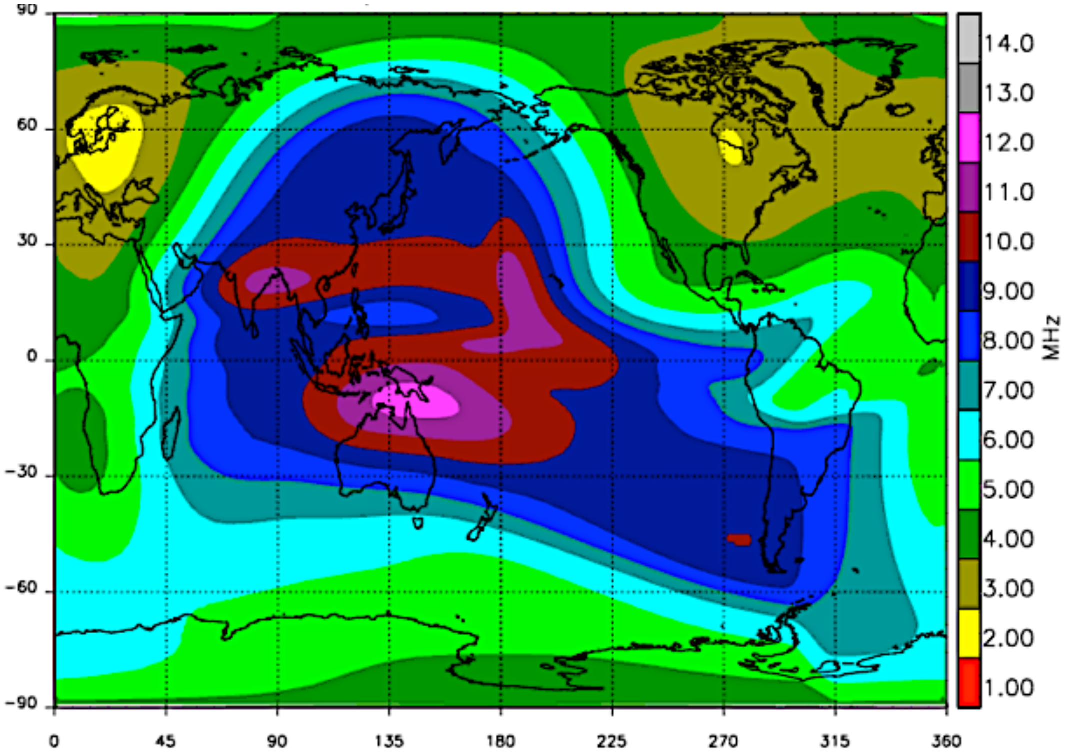

Copyright Commonwealth of Australia 2024, Bureau of Meteorology

Figure 9 Global critical frequency map for January 31, 2024 at 03:00 UT

Detailed regional critical frequency data is available on the www.skywave-radio.org website by clicking on Ionosonde under the Current Conditions tab. Data from a large number of ionosonde sites is available. For California the regional critical frequency data is obtained by clicking on Point Arguello, CA FoF2.

Figure 10 is the Point Arguello critical frequency chart also for Jan 31, 2024 @ 03:00 UT. This chart shows foF2 critical frequencies for the past 5 days (green traces), yesterday (red trace), and today (blue trace) in UT time. At this time and date the critical frequency at Point Arguello was approximately 4.5 MHz.

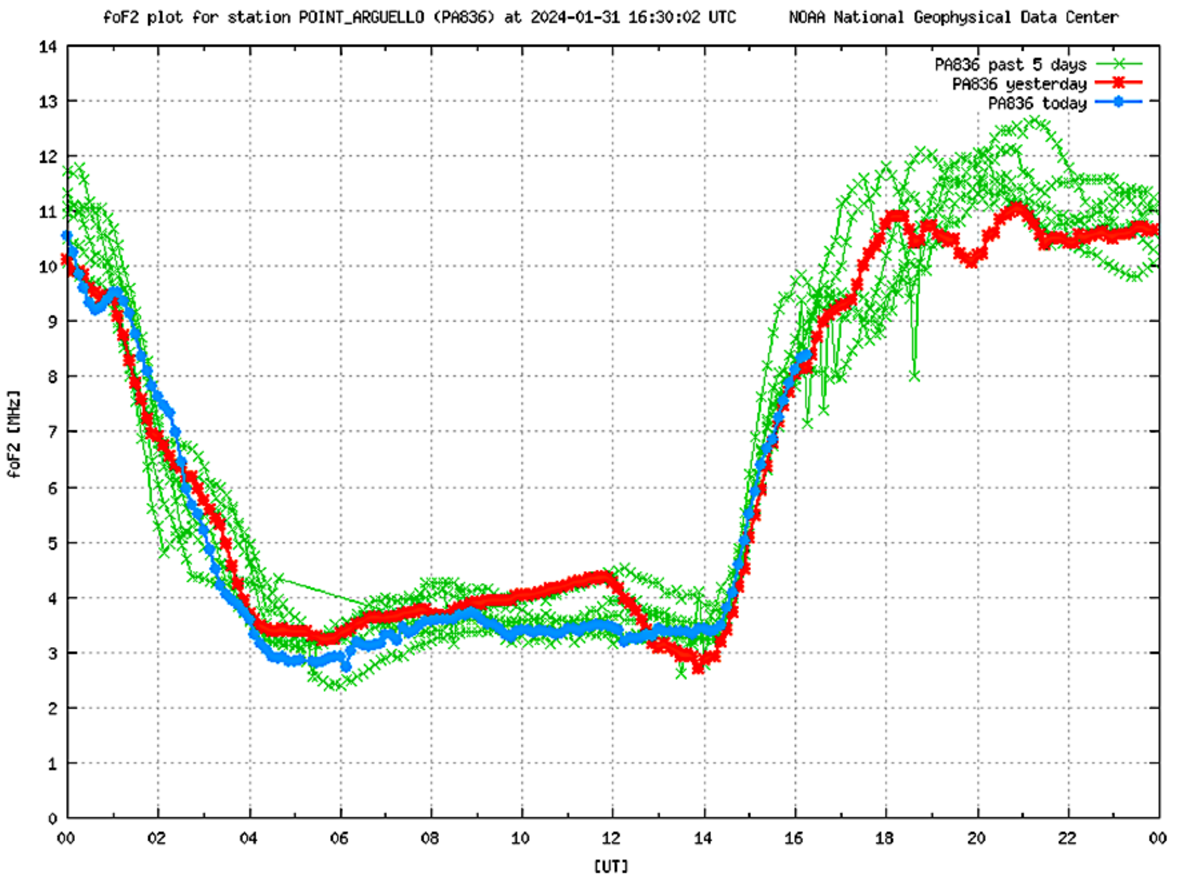

Figure 10 Point Arguello, California critical frequency for Jan 31, 2024 @ 03:00 UT

As illustrated above, critical frequencies change from one day to the next. The critical frequencies experienced today could well be different from those observed tomorrow. The changes in critical frequencies from one day to the next are attributed in part to:

- Daily changes in EUV radiation being received from the Sun,
- Occurrence of ionospheric storms caused by activity on the Sun,
- Ionospheric irregularities including Spread F Irregularities, Traveling Ionospheric Disturbances, and Thermospheric Winds, plus
- Changes in electrical currents flowing in the ionosphere.

A measure of the EUV radiation arriving from the Sun is provided by the Solar Flux Index (SFI). Solar flux is background solar radio noise caused by random collisions of electrons with heavier particles in the Sun's chromosphere and lower corona. The radio noise is measured daily by the Penticton Radio Observatory in British Columbia, Canada at a frequency of 2,800 MHz (10.7 cm wavelength). Solar Flux Index correlates well with measured levels of solar X-ray, EUV radiation, and sunspot numbers as illustrated in Figure 11. SFI numbers vary from below 50 during solar minimum to above 300 at the peak of a solar cycle. A high SFI number means a high F2 critical frequency and better HF communications. The current solar flux index is obtained by clicking on "NOAA Space Weather" under the "Current Conditions" tab of the www.skywave-radio.org web site.

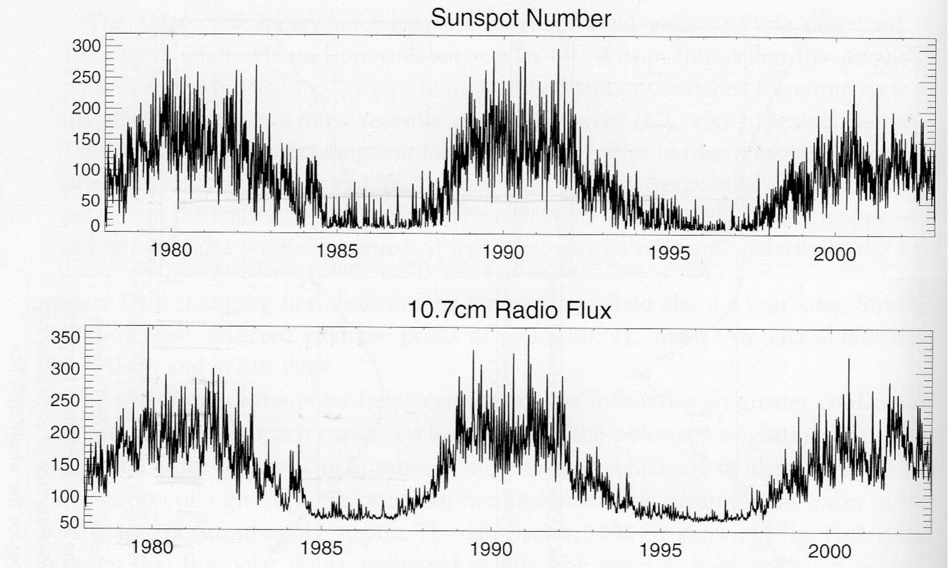

Figure 11 Radio Flux vs Sunspot Number (credit: G. deToma)

Critical frequencies are easily altered during the day and night by thermospheric winds which disrupt the wispy ionosphere continuously blowing it around.

The ionosphere is heated by excess photon energy above that necessary for ionizing neutral atoms and molecules. When a photon is absorbed by a neutral atom or molecule, energy in excess of that needed for ionization is transformed into the kinetic energy of the escaping electron as it speeds away from its parent atom or molecule. The higher the kinetic energy the greater the energy released in the form of heat when the electron collides with an atom or molecule. Because of this heating the ionosphere is hotter than the surrounding neutral atmosphere affecting the vertical distribution of plasma in the ionosphere's F2 region.

During ionospheric storms solar wind particles (electrons, protons, and some alpha particles) stream down into the high latitude auroral atmosphere. Collisions of these particles with neutral atoms and molecules change the chemical composition of the auroral ionosphere, heat the atmosphere, and change the circulation patterns of thermospheric wind. Heating plus changes in chemical composition accelerates the recombination of electrons with ions, decreasing electron densities in the auroral ionosphere. Convection currents carry the electron depleted auroral plasma down into mid latitudes causing F2 layer critical frequencies to drop by a factor of 2 or more. The drop in critical frequency impacts the higher HF bands more than lower frequencies. Radio frequencies from 20 through 10 meters are affected the most. These bands often disrupted for a week or more.

15.3.2 Seasonal Variations in Critical Frequencies

Seasonal changes in critical frequencies are due primarily to:

- Changes in zenith angles, and
- Changes in the Earth’s upper atmosphere.

Noon time zenith angles are always less in summer when the Sun is more overhead. We would thus expect critical frequencies to be higher in summer than in the winter. And they are for the E and F1 zones, but not so for the F2 region. During solar maximum F2 critical frequencies are substantially higher in winter than in summer, as illustrated in Figure 12, despite the fact that in winter the Sun is low in the sky. This is known as the seasonal anomaly.

As expected, E region critical frequencies are slightly higher in summer during both solar maximum and minimum. F1 critical frequencies are also higher in the summer during solar minimum. However, during solar maximum the F1 region is present only in the summer. It disappears in winter.

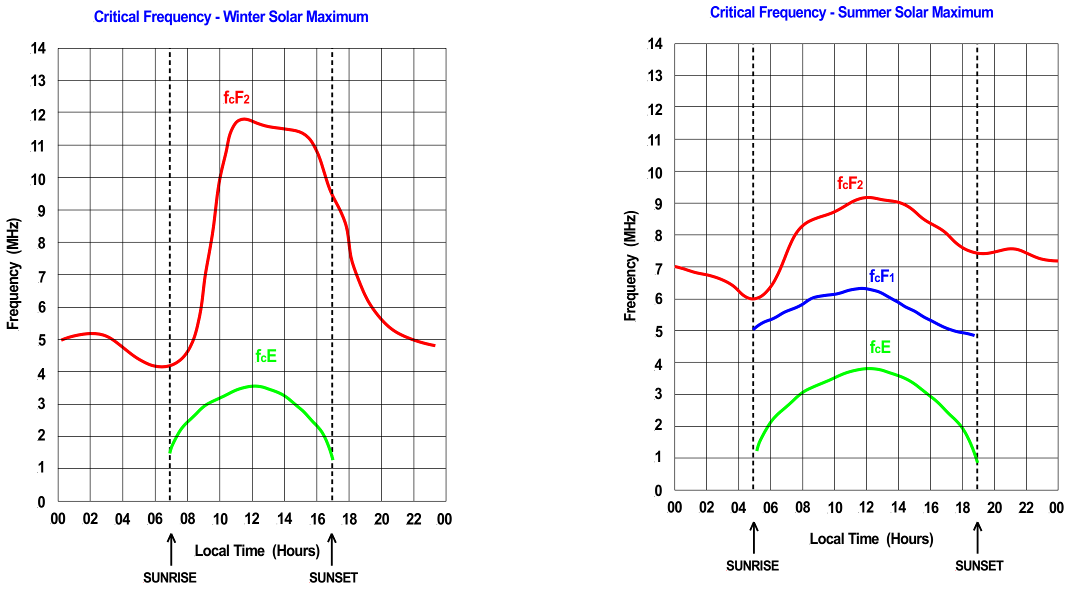

Figure 12 Winter and summer critical frequencies during solar maximum (source: author)

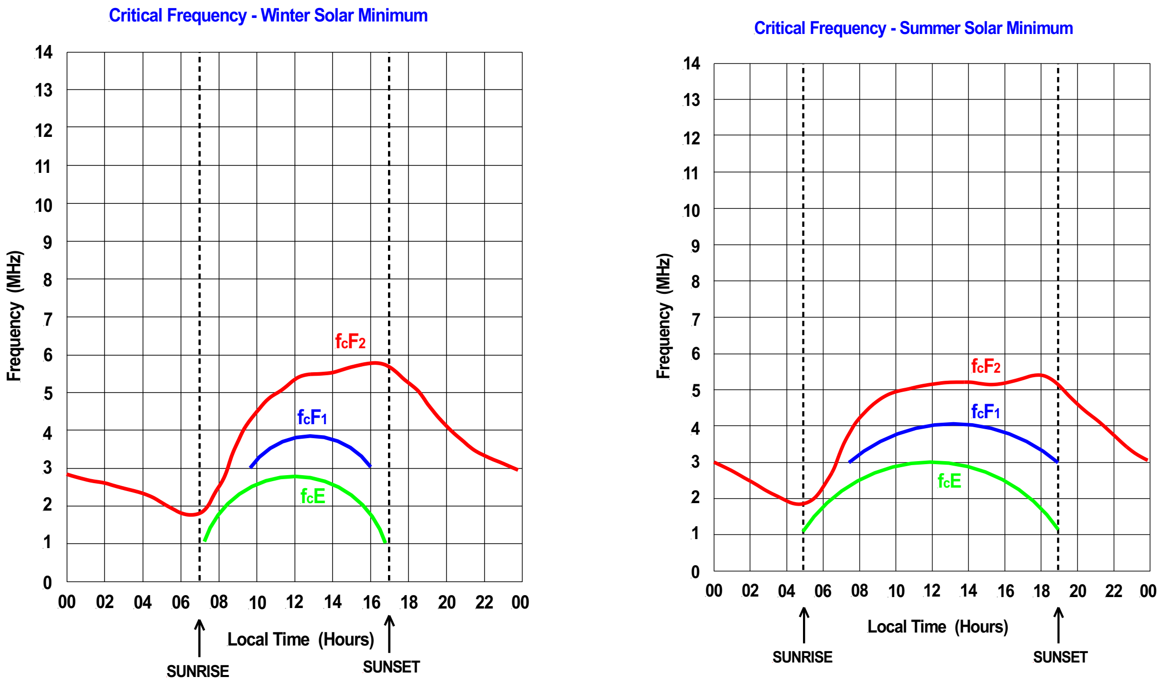

Figure 13 Winter and summer critical frequencies during solar minimum (source: author)

All critical frequencies are lower during solar minimum as illustrated in Figure 13. Low activity on the Sun means lower levels of EUV radiation available for ionizing Earth's upper atmosphere. In addition, during solar minimum F2 critical frequencies tends to peak in the late afternoon instead of around noon time. This is not what would be expected, but it is what happens. The F1 region appears in both the winter and summer during solar minimum.

Seasonal variations in F2 critical frequencies can be explained in part by changes in upper atmosphere chemical reaction rates plus changes in the ratios of major atmospheric species.

Reaction rates are generally temperature sensitive. For example, the first step in the dissociative recombination of an oxygen ion O^+ with a nitrogen molecule N_2 is

$$O^+ + N_2 \rightarrow NO^+ + N$$

This reaction varies considerably with the temperature of neutral nitrogen N_2. The reaction rate increases by a factor of 16 for a times 4 increase in temperature. Changes in reaction rates contributes to both the F2 seasonal anomaly and persistence of the F region at night. During summer the higher temperature of N_2 increases the rate of dissociative recombination resulting in lower electron concentrations and lower F2 critical frequencies than in the winter. At night cooler temperatures slow down the recombination process causing the F region to remain at least partially ionized.

Electron production rates in the F2 region depends on the concentration of atomic oxygen O while the recombination rate is controlled by concentrations of N_2 and O_2. Oxygen atoms are the species most heavily ionized in the F2 region by high energy EUV radiation. An increase in atomic oxygen relative to molecular nitrogen and oxygen increases electron density. Thus, the ratio of atomic oxygen to molecular oxygen O/O_2 and atomic oxygen to molecular nitrogen O/N_2 is important. The ratio O/N_2 at an altitude of 300 km is about 6 in winter and around 2 in the summer, again resulting in lower electron densities and lower F2 critical frequencies in the summer compared to winter.

15.3.3 Variations In Critical Frequencies Over An 11 Year Solar Cycle

The EUV radiation responsible for ionizing Earth's upper atmosphere accounts for only 0.001% of the Sun's total energy output as illustrated in Figure 14. While the Sun's output remains incredibly stable over thousands of years, the Sun's EUV energy output is not stable at all! EUV energy varies considerably over the 11-year solar cycle. Consequently, the level of ionization in Earth's upper atmosphere also varies over the same time period. EUV energy output is greatest during solar maximum when there are large numbers of sunspots and lowest during solar minimum when there are few if any sunspots.

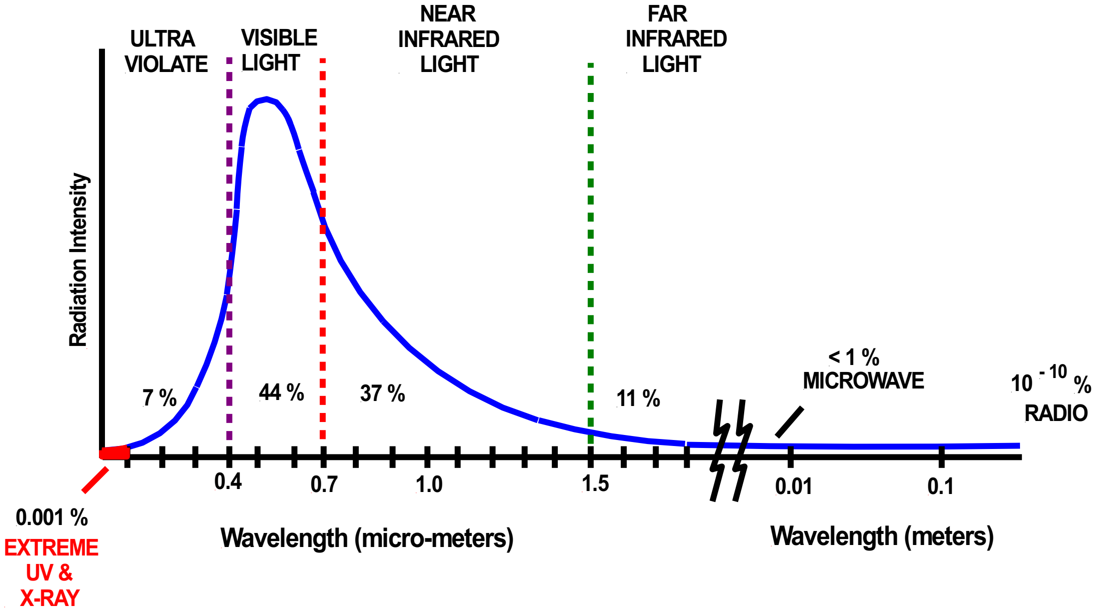

Figure 14 Sun's energy output (source: author)

The solar cycle is the result of the Sun's magnetic field being created near its surface, instead of deep within the Sun, coupled with the Sun's differential rotation. The Sun's equator rotates in 24.5 days while the poles rotate in 34 days. The Sun's differential rotation causes its magnetic field to become badly twisted and distorted.

At sunspot minimum the Sun’s magnetic field, shown in Figure 15a, is a “quiet” north – south bipolar field similar to that of Earth’s magnetic field. The strength of Earth’s magnetic field is around 0.2 gauss. At sunspot minimum the strength of the Sun’s magnetic field is about 1.0 gauss. The Sun’s quiet magnetic field is not that much different from Earth’s magnetic field. Sunspot minimum for Solar Cycle 24 occurred in 2008 (Figure 16)

Over 3 years or so the Sun’s differential rotation slowly drags and winds the magnetic field around the Sun as illustrated in Figure 15b. This is known as the ascending phase of the solar cycle. For Solar Cycle 24 the ascending phase occurred from 2009 to around 2012.

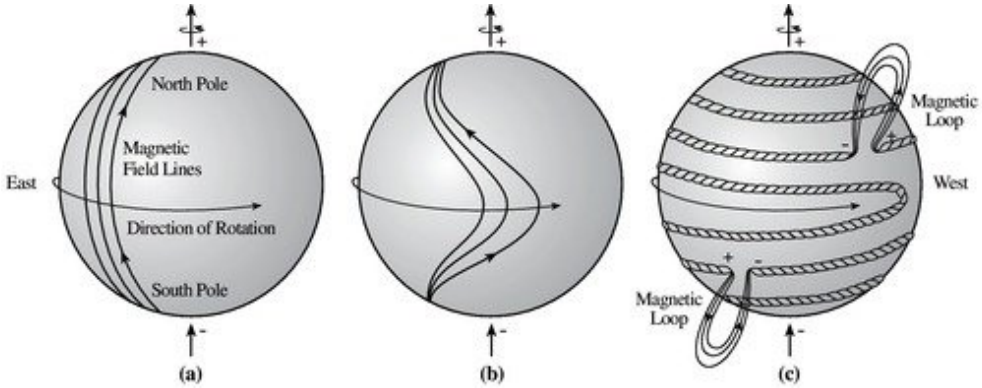

Figure 15 Magnetic field lines become wrapped and twisted around the Sun
(credit: NASA’s Cosmos – ase.tufts.edu)

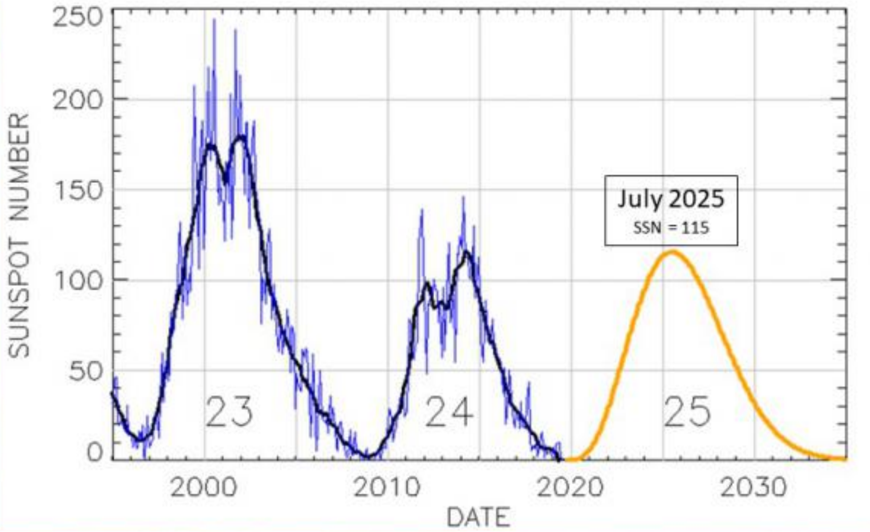

Figure 16 Solar Cycles 23 and 24 (credit: NOAA Space Weather Prediction Center)

Differential rotation winds the magnetic field around the Sun in tighter ever-increasing number of turns (Figure 15c). In addition, convection zone turbulence just below the Sun's surface twists the magnetic field lines into ropes some of which become knotted. This is not a sustainable process. Something has to break, and it does! Continued winding, twisting, and knotting creates tremendous stress in the magnetic field driving field intensities to well over 3,000 gauss. The enormous stress eventually causes the field to rupture in many places across the Sun. As it does so sunspots, high arching coronal loops, and solar flares erupt from the Sun (Figure 17). The number of sunspots visible on the Sun reaches a maximum during this very turbulent period. This is solar maximum. Solar maximum for Solar Cycle 24 occurred from 2011 to 2015.

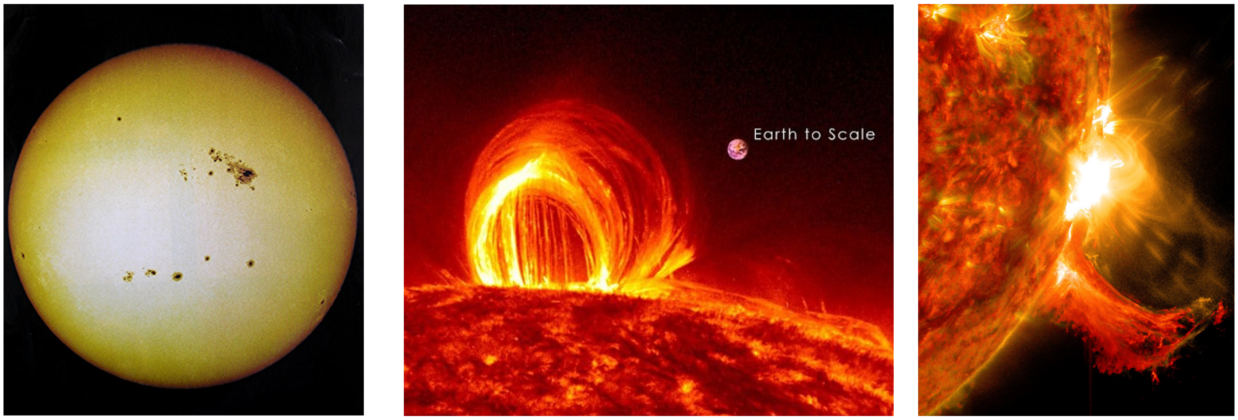

Sunspots Coronal Loop Solar Flare

Figure 17 Sun during solar maximum (source: NASA Goddard Space Flight Center)

Rupturing of the magnetic field causes it to disintegrate. As it disintegrates, the magnetic field unwinds, solar activity subsides, and sunspots gradually disappear. This is the declining phase of the solar cycle which for Solar Cycle 24 occurred from 2015 to 2019. In 2019 the number of visible sunspots reached zero defining the next solar minimum and the end of Solar Cycle 24.

Sunspots, like the one shown in Figure 18, occur at locations on the Sun where strong magnetic fields erupt through the photosphere (the photosphere is the yellow regions in Figure 18). The magnetic fields suppress the upward flow of hot plasma from deep in the Sun's convection zone. Starved of hot plasma, a sunspot is cooler than the surrounding photosphere which gives a sunspot its black appearance.

Associated with sunspots are hot bright irregularly shaped areas called plages (white regions in Figure 19). Plages are important because they emit copious amounts of EUV radiation responsible for ionizing Earth's upper atmosphere. Plages are formed in the chromosphere by intense magnetic fields radiating out from the photosphere. They occur in active sunspot regions of the Sun and usually form several days prior to sunspots in the area. In addition, plages typically last longer than their associated sunspots.

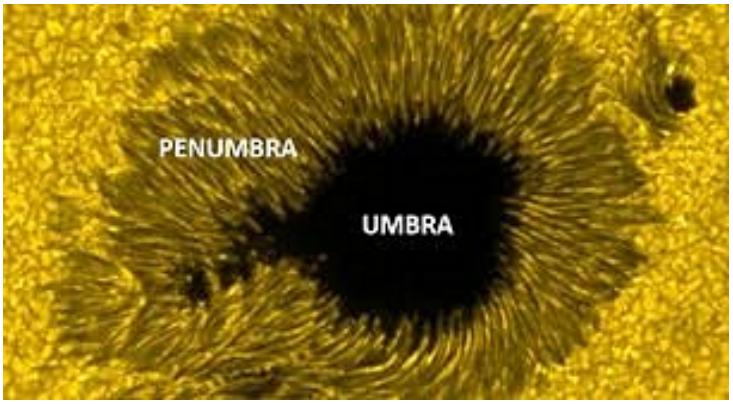

Figure 18 A closer look at sunspots (credit: spaceweatherlive.com)

While there is a strong correlation between sunspots and long-distance radio communications, it turns out that sunspots have little to do with HF propagation. Sunspots are far too low in temperature to generate the EUV radiation needed to ionize Earth's upper atmosphere. The required EUV radiation is primarily produced by plages. The problem is that plages cannot be seen (without special equipment) because of the intense light emanating from the photosphere. The photosphere is simply too bright. But sunspots can easily be seen as readily apparent in Figure 17. Thus, sunspots become markers for plages. A large number of sunspots means a large number of plages, high EUV levels, strong ionization of the Earth's ionosphere, and good HF radio communications. When they are present, the extreme heat generated by coronal loops also emits copious amounts of EUV radiation.

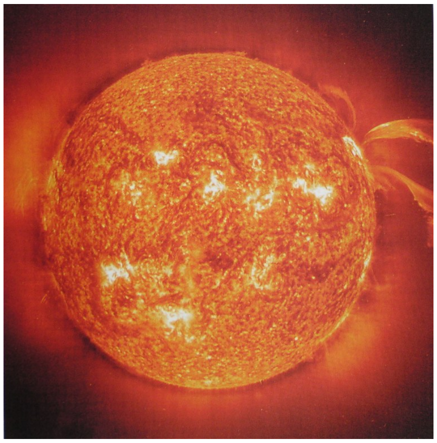

Figure 19 Sun's chromosphere shown in H alpha (H_α) light (credit: universitytoday.com)

The E, F1, and F2 critical frequencies all vary with the solar cycle as shown in Figure 20. This is to be expected. An increase in solar activity produces an increase in EUV radiation responsible for ionizing Earth's upper atmosphere.

The red trace in Figure 20 is the smoothed sunspot number (ssn) for the years 1988 through 2015. The smoothed sunspot number is the number of sunspots observed averaged over a 13-month period. The vertical scale on the right is the smoothed sunspot number. The scale on the left is critical frequency in MHz. The graph shows three solar cycles. The solar cycles on the right and left are partial solar cycles while the complete Solar Cycle 23 is shown in the middle. Solar Cycle 23 began as a minimum in late 1996 with sunspot numbers around 10 or so. Sunspot maximum occurred in mid 2000 and again in 2002 before declining to the next solar minimum in 2009.

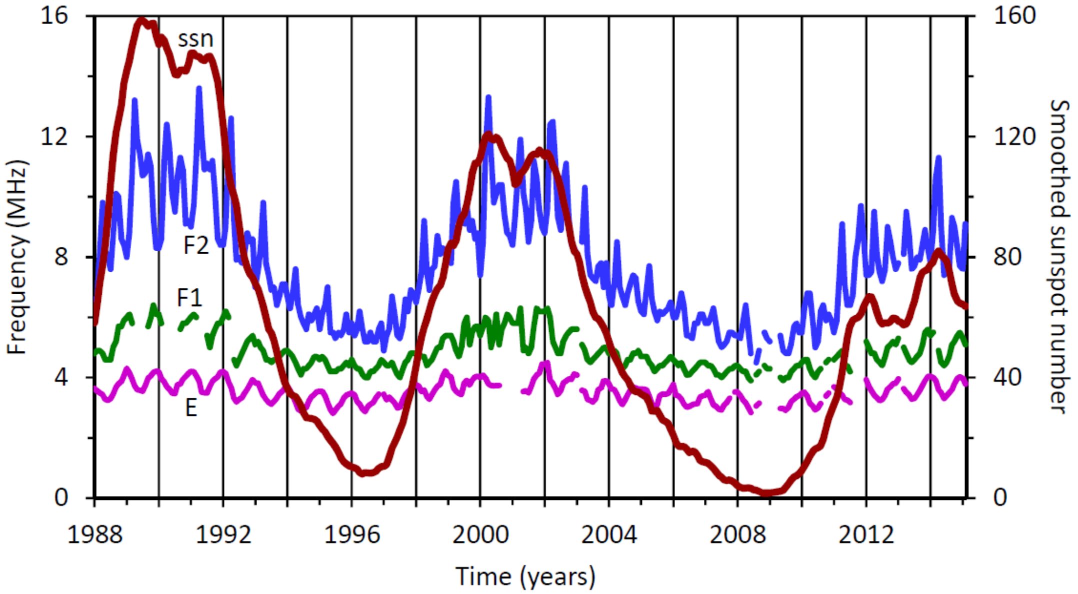

Figure 20 Critical frequency variations with the solar cycle (source: sws.bom.gov.au)

As can be seen in Figure 20, the solar cycle has the greatest effect on F2 critical frequencies. The highest F2 critical frequencies occur during solar maximums with critical frequencies typically ranging from 8 to 14 MHz. At solar minimum the typical F2 critical frequency range is 5 to 6 MHz. The highest F1 and E critical frequencies also occur during solar maximum. However, the solar cycle has less of an effect on F1 and E critical frequencies with the E region critical frequency being affected the least.

In general, solar EUV radiation changes by a factor of 10 over the course of an 11-year solar cycle as illustrated in Figure 21. In this figure the vertical axis is the percent change in EUV radiation from solar maximum to solar minimum. The horizontal axis is EUV wavelength. The graph shows the percent difference between solar maximum and minimum EUV radiation is greatest for high energy short wavelength EUV radiation. This accounts for the solar cycle having a greater effect on the F2 region of the ionosphere than on the E region. The F2 region is formed by high energy EUV radiation in the range from 20 to 90 nm ionizing individual oxygen atoms forming O^+ ions. This is the range of EUV radiation most effected by the solar cycle. In contrast, the E region is formed by lower energy EUV radiation in the range from 80 to 103 nm that ionizes molecular oxygen O_2 to form O_2^+ ions. In addition, lower recombination rates in the F2 region, coupled with electrons and ions drifting up from the F1 into the F2 region, accentuates the F2 region variation with the solar cycle.

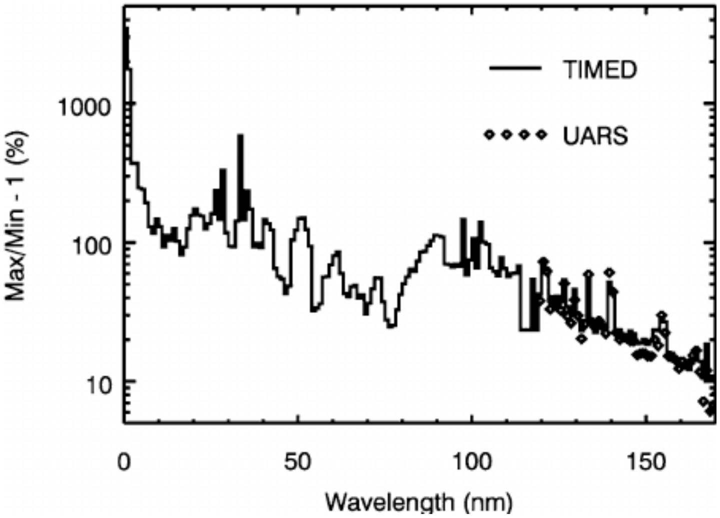

Figure 21 Solar cycle EUV variation vs wavelength (source: ResearchGate)

15.4 Ionospheric Sounding

Ground based sounders, known as ionosondes Figure 22, have been used since the early days of radio to probe the ionosphere. They have provided the bulk of our current information on ionospheric structure.

Figure 22 Ionosonde controller and data processor (source: Electronics Notes)

15.4.1 Ionosonde systems

A typical ionosonde system is shown in Figure 23. An ionosonde transmits a pulsed signal straight up into the atmosphere and receives an echo, or reflection, of the signal back from the ionosphere. The condition of the echoed signal, whether it is reflected or not, the width and frequency of the reflected pulse, and the time between transmission and reception provides information on the current condition of the ionosphere. The time between transmission and reception of a pulse indicates the height at which the signal was reflected.

An ionosonde utilizes a sweep frequency transmitter. The transmitter is driven by the ionosonde processor which sends a long series of pulses each at a slightly different frequency. The pulses are transmitted over a frequency range of typically 0.5 to 25 MHz.

A radio signal transmitted vertically will propagate through the ionosphere until it reaches an altitude at which its frequency equals the ionosphere plasma frequency. At that point it is reflected back to ground.

The ionosonde processor tunes the receiver to the frequency of the transmitted signal. Echoes of the transmitted pulse are received by the receiver and sent to the processor.

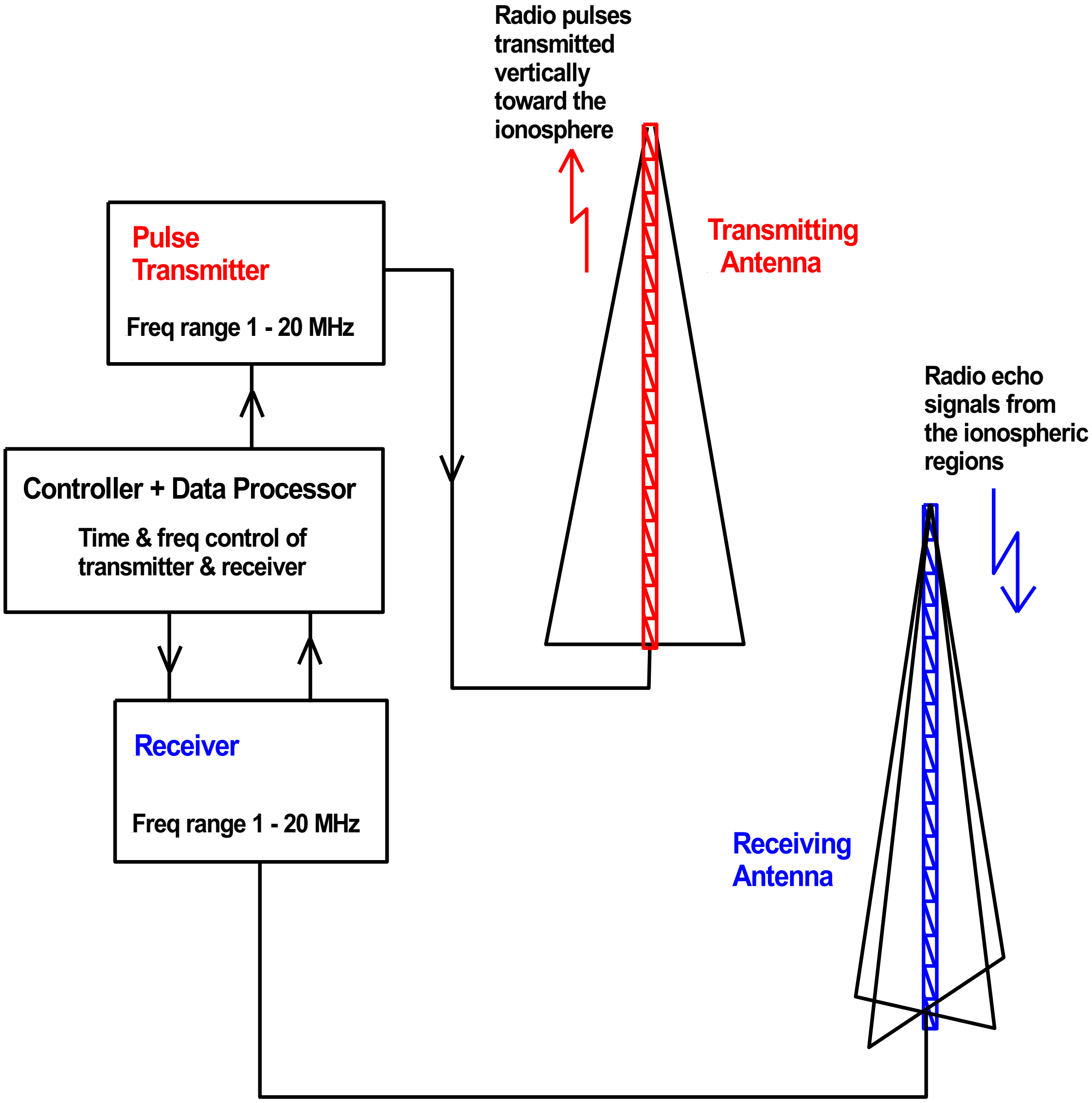

Figure 23 Ionosonde system diagram (source: spaceacademy.net.au)

The processor converts the received echoes into a graphical display of echo time delay verses frequency. The display is known as an ionogram. On the ionogram, echo delay is converted to altitude of the reflection point using the equation

$$\text{Altitude km} = (1/2)\, c\, T$$

where

c = speed of light

T = time delay between transmission and reception of a pulse.

The factor 1/2 appears in the equation because T is the total round-trip time to the reflection point and back again. The time from the transmitter to the reflection point is one half that (1/2 T).

For example, in the ionogram shown in Figure 24 a signal reflected at a frequency of ~ 3MHz indicating the presence of an E region. A 4.2 MHz signal passes through the E region and is reflected by the F1 layer identified by the longer time between transmission and reception of the pulse. A 5.1 MHz signal passes through both E and F1 before being reflected in the F2 region, represented by a still longer delay. In this example a 7 MHz pulse passes through all 3 layers without being reflected and is lost to outer space.

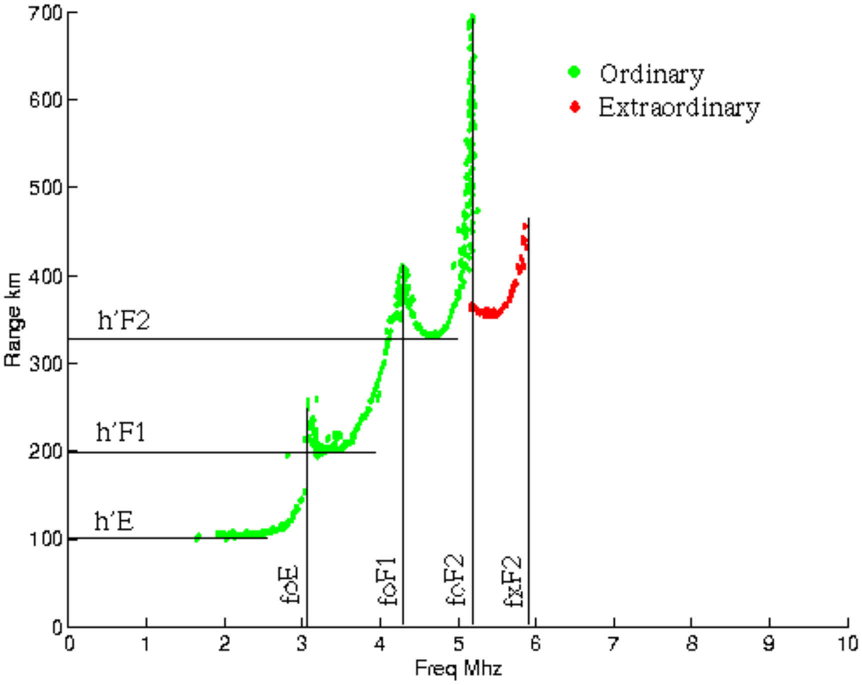

Figure 24 Ionogram graphical display (source: ukssddc.ac.uk)

15.4.2 Ordinary and Extra Ordinary Modes

Earth's geomagnetic field causes a HF radio signal to split into two different signals as it enters the ionosphere. The two signals each have a slightly different mode of propagation through the ionosphere (slightly different indices of refraction resulting in slightly different velocities, reflection heights, and direction of travel). One propagation mode is termed the ordinary or o-mode. The other is called the extraordinary mode, or x-mode. Consequently, each ionogram consists of two traces, one corresponding to the o-mode (red trace) and the other to the x-mode (green trace) in Figure 25. At a frequency of 4 MHz in Figure 25 the o-mode signal reflects at a lower altitude than the x-mode (230 vs 250 km). At a frequency of 7 MHz the situation is reversed. At 7 MHz the x-mode reflects at 280 km while the o-mode reflects at 340 km. Because of the higher reflection altitude, the 7 MHz hop distance for the o-mode signal is longer than the x-mode signal.

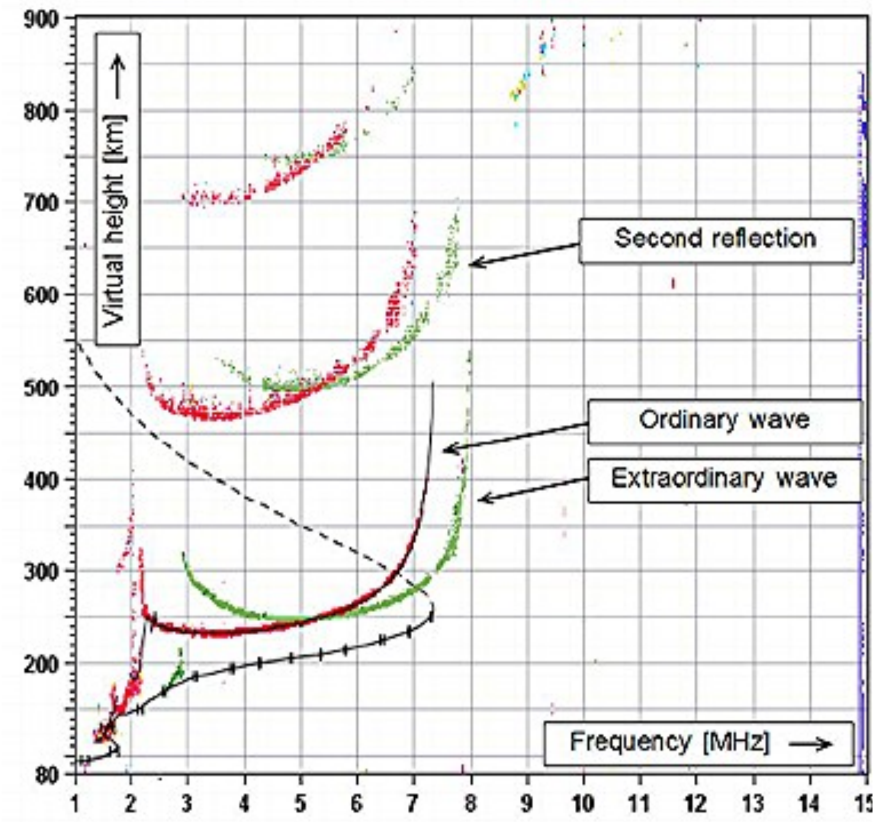

Figure 25 Ionogram showing both ordinary and extra ordinary modes (source: ResearchGate)

15.4.3 Reading an Ionogram

By convention the o-mode trace is used in determining the critical frequencies and maximum electron densities at the points of reflection. The o-mode (f_o) critical frequency f_oF2 is

$$f_oF2 = 9(10^{-3})\sqrt{N_{max}}$$

where N_{max} is the maximum electron density and f_oF2 is read from the ionogram. From this information the maximum electron density N_{max} in the F2 region can be calculated from

$$N_{max} = \left[\frac{f_oF2}{9(10^{-3})}\right]^2$$

In Figure 26, f_oF2 is the o-mode F2 critical frequency and f_xF2 is the x-mode F2 critical frequency. h’F2 is the height (altitude) of the F2 maximum electron density.

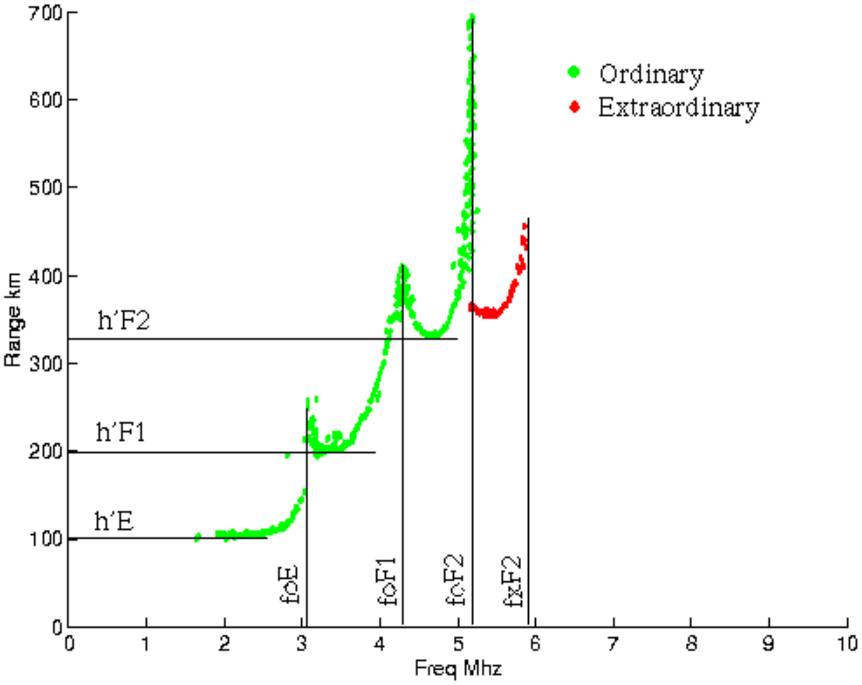

Figure 26 Ionogram graphical display (source: ukssddc.ac.uk)

The signal transmitted from the ionosonde is assumed to travel at the speed of light c. However, this is not really the case. The speed of a signal transmitted through the ionosphere is actually less than the speed of light. In addition, its speed varies as the ionosphere’s electron density changes with altitude. The speed decreases significantly as the transmitter’s sweep frequency approachs a critical frequency point, considerably increasing the reflection time T at that point. On an ionogram, the increase in T appears as a spike in the height at which critical frequency reflection occurs. This is an artifact. The reflection heights are actually h’E, h’F1, and h’F2 as shown in Figure 26. However, the spikes make it easy to identify the critical frequency points.

15.4.4 Types of Ionosondes

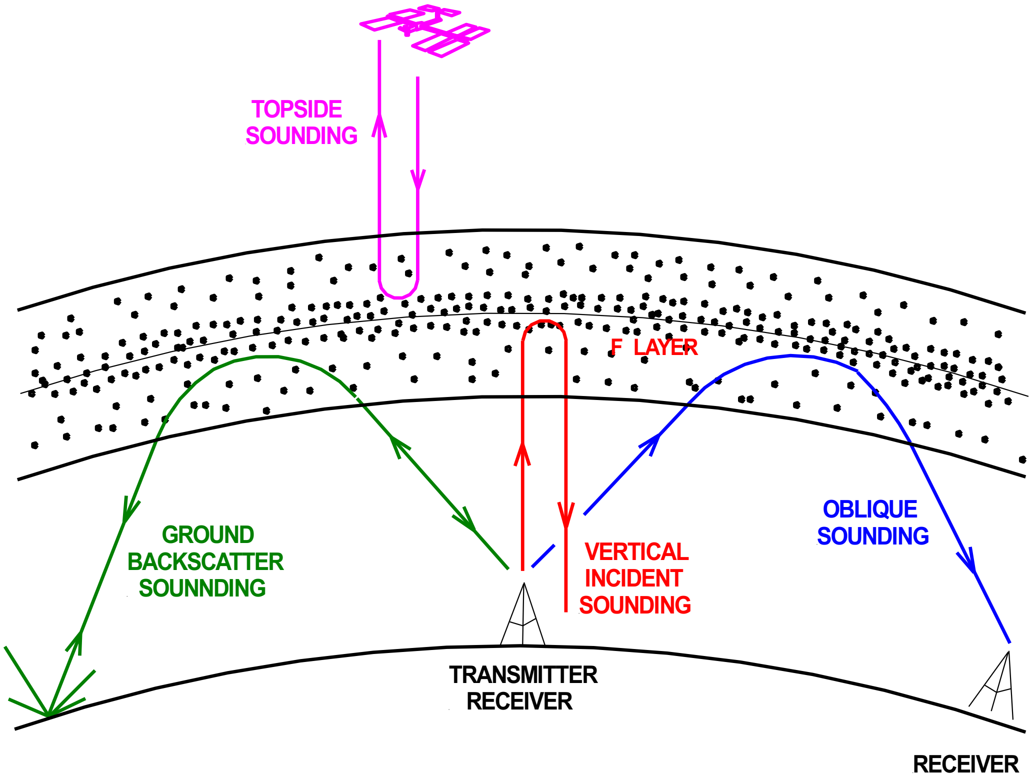

Figure 27 Types of ionosphere sounding (source: author)

Several types of ionosonde sounders (also known as HF radar) are currently in use. These are illustrated in Figure 27. They include:

- Vertical incident sounders (VIS),
- Oblique sounders,
- Direct and ground backscatter radar, and
- Topside sounding using Earth satellites.

15.4.4.1 Vertical Incident Sounders (VIS)

Vertical incident sounders (VIS) transmit a sweep frequency HF signal vertically into the atmosphere and receive the echoes from the ionosphere on a co-located receiver as illustrated in

Figures 23, 27 and 28. Vertical incident sounding is the earliest method used for investigating the ionosphere. Over the years it has provided a very complete picture of ionospheric structure. It remains the primary method for determining current ionospheric conditions in the E, F1, and F2 regions. However, determining current D region conditions is a problem. Because of D region signal absorption, special methods are needed to determine electron densities in this region.

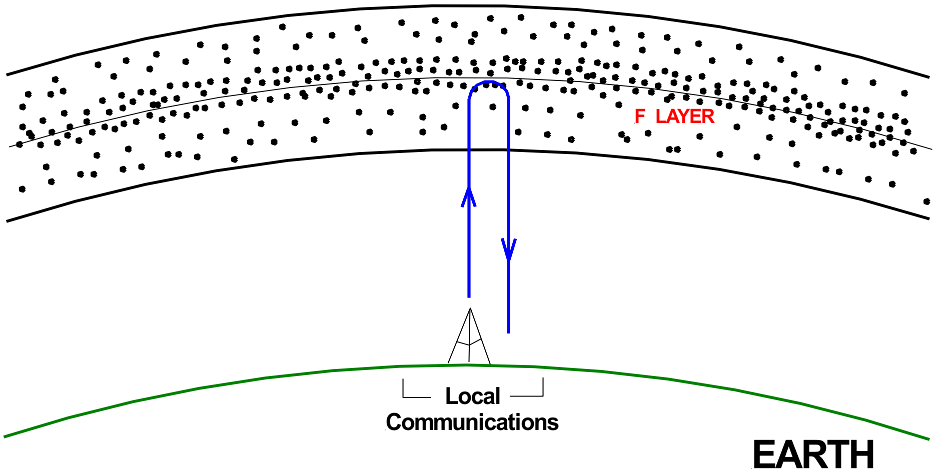

Figure 28 Vertical Incident Sounding (source: author)

Much of the current ionospheric nomenclature has evolved from the early VIS investigations. Typical VIS specifications include:

Frequency	0.5 to 25 MHz
Power	300 W to 10 KW
Sweep Cycle	30 sec – 5 min.
Pulse Rate	50 per second
Pulse Width	30 microseconds

15.4.4.2 Oblique Sounding

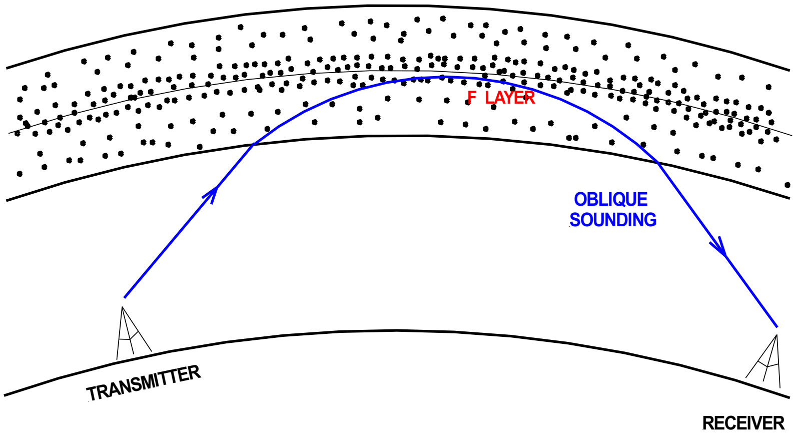

Figure 29 Oblique Sounding (source: author)

Oblique sounding monitors propagation conditions on an HF communications circuit between two locations as illustrated in Figures 27 and 29. This is done by transmitting pulses of radio energy obliquely through the ionosphere from a sweep frequency transmitter to a distant receiver. The transmitter and receiver must be synchronized in order to produce an oblique ionogram. Oblique sounding is very important for real time radio frequency management. It is used to determine which frequencies and propagation modes are available over a particular communications circuit at the time of operation. It is also very important for testing propagation predictions and validating ionospheric models. Monitoring HF broadcast transmitters such as WWV, WWVH, and W1AW transmissions is a form of passive oblique sounding. The receiving station can determine current HF conditions by monitoring the strength and stability of the broadcast station.

15.4.4.3 Backscatter HF Radar

Signals transmitted into the ionosphere are often scattered by ionospheric irregularities. Some of the scattered signal is received back at the transmitting site as illustrated in Figures 27 and 30. Two types of backscatter HF radar systems are in use. They are:

- Direct Backscatter Radar, and
- Ground Backscatter Radar

Both types are used to study ionospheric irregularities. Backscatter HF Radars are typically expensive complex systems frequently utilizing large arrays of up to 16 log-periodic antennas. Interpretation of backscatter data is often complex.

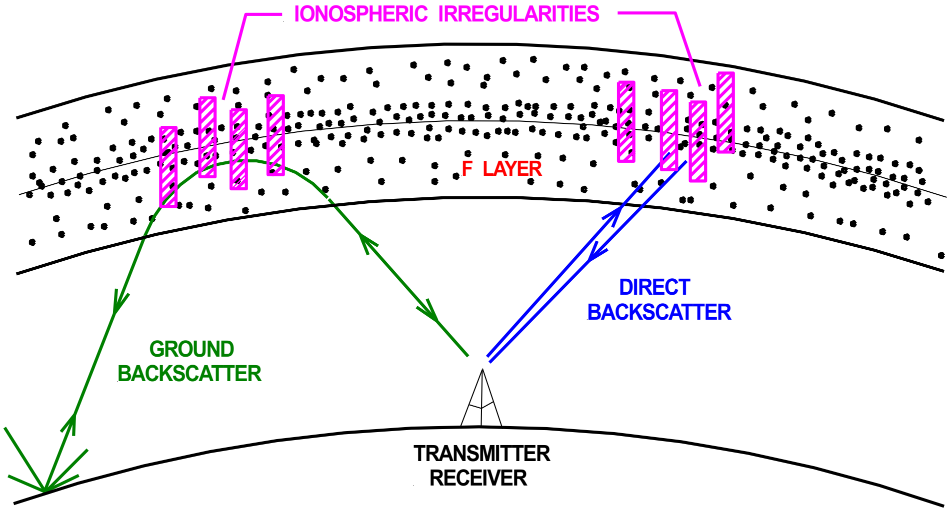

Figure 30 Backscatter HF Radar (source: author)

Direct backscatter HF radar are systems designed to make use of the backscatter phenomena to study ionospheric irregularities by analyzing the received backscattered signal. Networks of direct backscatter systems are used to study the high latitude ionosphere. All of the north polar region is covered by direct backscatter systems and part of the south polar region.

Signals refracted back to Earth by the ionosphere scatter when they hit the ground. A small amount of scattered energy usually travels back through the ionosphere to the transmitting site. The returning signal (ground echo) is often distorted by ionospheric irregularities. These irregularities are studied by analyzing the distorted ground echo. Ground backscatter signals are orders of magnitude weaker than direct backscatter signals.

15.4.4.4 Top Side Sounding

Top side sounding utilizes Earth satellites to probe the upper part of the ionosphere as illustrated in Figure 31.

Ground based ionosondes can only “see” the bottom of the ionosphere. Signals transmitted vertically at the F2 critical frequency fcF2 can observe the ionosphere up to the F2 region’s maximum ionization level. Vertical signals transmitted at higher frequencies pass through the ionosphere without being reflected back to Earth, and thus provide no information.

Top side sounding from an Earth satellite is very similar to ground-based VIS except it probes down into the ionosphere from above. The F2 maximum ionization level is the furthest that a top side sounder can see down into the ionosphere, again by transmitting at frequencies at and below the F2 critical frequency fcF2. Transmitting at a higher frequency will cause the signal to pass through the ionosphere to the Earth instead of being reflected back to the satellite. Consequently, top side sounders explore the ionosphere from the F2 maximum ionization level to an altitudes of 1,000 km or more

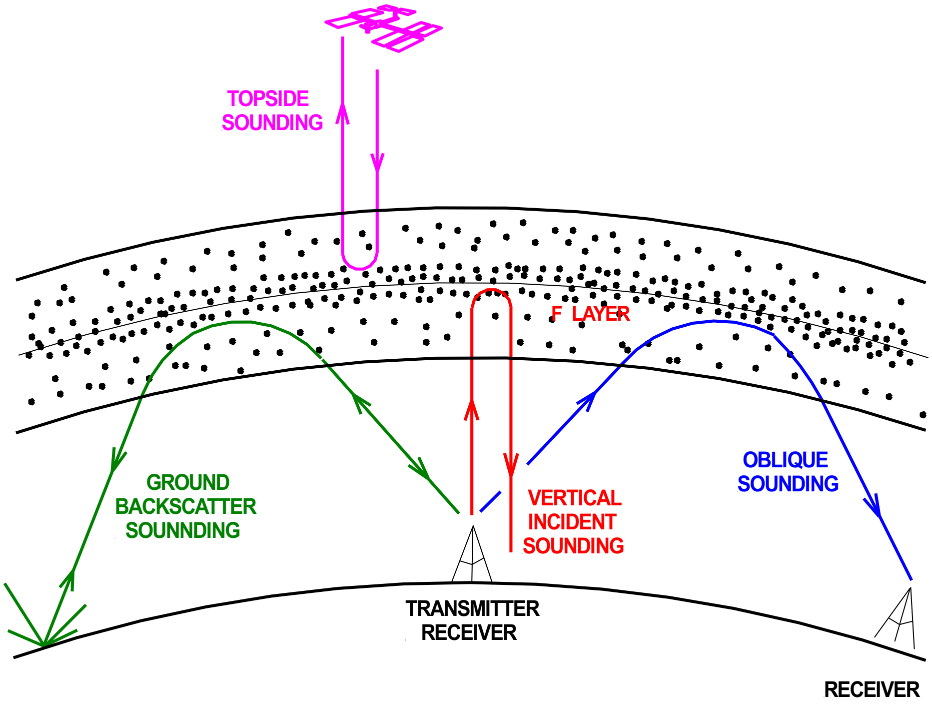

Figure 31 Top Side Sounding (source: author)

References

Hunsucker R. D.; Hargreaves, J. K.; "The High-Latitude Ionosphere and its Effects on Radio Propagation"; Cambridge University Press 2003

Davies, Kenneth; "Ionospheric Radio"; Peter Peregrinus Ltd.,1990

McNamara, Leo F.; "The Ionosphere: Communications, Surveillance, and Direction Finding"; Krieger Publishing Company, 1991

Nichols, Eric P.; "Propagation and Radio Science"; The American Radio Relay League, Inc. 2015

Yeang, Chen-Pang; "Probing The Sky With Radio Waves"; The University of Chicago Press, 2013

Devoldere, John; "Low-Band DXing" fourth edition; ARRL, 2005

Levis, Curt A. ; Johnson, Joel T.; and Teixeira, Fernando L.; "Radiowave Propagation Physics and Applications"; John Wiley & Sons, Inc., 2010

Ahrens, C. Donald; "Essentials of Meteorology"; Wadsworth Publishing Company, 1998

UCAR Center for Science Education (UCAR SciEd); https://scied.ucar.edu/learning-zone/atmosphere/

Khazanov, George V.; "Space Weather Fundamentals"; CRC Press, 2016

Foukal, Peter; "Solar Astrophysics third edition"; Whiley-VCH Publishing Company, 2013

Ganushkina, N. Yu.; Liemohn, M. W.; Dubyagin. S.; "Current Systems in the Earth's Magnetosphere"; AGU, March 8, 2018

Gallagher, Dr. D.L.; "The Earth's Plasmasphere"; Space Plasma Physics, Marshall Space Flight Center, Huntsville, Al, September 05, 2018

Moore, T. E., Morwitz, J. L.; "Stellar Ablation of Planetary Atmospheres"; August 9, 2007

Yau, Andrew W.; Abe, Takumi; Peterson, W. K.; "The Polar Wind: recent Observations"; Department of Physics and Astronomy, University of Calgary

Carroll, Bradley W. and Ostlie, Dale A.; "An Introduction to Modern Astrophysics"; Addison-Wesley Publishing Company Inc., 1996

Goodman, John M.; “Space Weather & Telecommunications”; Springer Science+Business Media Inc. 2005

Cander, Ljiljana R.; “Ionospheric Space Weather”; Springer Nature Switzerland AG 2019

Moldwin, Mark; “An Introduction to Space Weather”; Cambridge University Press, 2008

Campbell, Wallace H.; “Introduction to Geomagnetic Fields”; Cambridge University Press, 2003

Golub, Leon and Pasachoff, Jay M.; “Nearest Star The Surprising Science of Our Sun second edition”; Cambridge University Press, 2014

Loff, Sarah: ”Explorer and Early Satellites”; National Aeronautics and Space Administration, Aug 3, 2017

Minzner, R. A.; “The 1976 Standard Atmosphere Above 86 km Altitude” NASA Goddard Space Flight Center, 1976